Solid-State Characterization of Candesartan Cilexetil (TCV-116): Crystal Structure and Molecular Mobility

Hirokazu MATSUNAGA,*[,a] Taro EGUCHI,[b] Koji NISHIJIMA,[a] Toshio ENOMOTO,[a] Kazumichi SASAOKI,[a] and Nobuo NAKAMURA[b]

Drug Analysis & Pharmacokinetics Research Laboratories, Takeda Chemical Industries, Ltd.,[a] 17–85 Juso-honmachi 2-chome, Yodogawa-ku, Osaka 532–8686, Japan and Department of Chemistry, Graduate School of Science, Osaka University,[b] 1–16 Machikaneyama-cho, Toyonaka-shi, Osaka 560–0043, Japan.

Received August 13, 1998; accepted November 19, 1998

Two polymorphs (form I, form II) and amorphous form of candesartan cilexetil ((±)-1-(cyclohexyloxycarbonyloxy)ethyl 2-ethoxy-1-[[2′-(1*H*-tetrazol-5-yl)biphenyl-4-yl]methyl]-1*H*-benzimidazole-7-carboxylate; TCV-116) were characterized by differential scanning calorimetry (DSC), powder X-ray diffractometry (XRD), IR spectroscopy, and solid-state NMR. The molecular motion of TCV-116 in three forms was investigated by solid-state NMR, and signals due to the terminal cyclohexane ring of TCV-116 in form II were affected by temperature, whereas those in form I were scarcely affected. At lower (−89 °C) and higher temperature (80 °C), sharp signals due to the cyclohexane ring in form II were observed, whereas shallow signals were observed in the medium temperature range. These results indicated that the cyclohexane ring in form II presumably existed as the stable conformer: the chair form at lower temperature, and the chair form–chair form conformational change occurred at higher temperature. At the medium temperature, the broad and weak signals assigned to the cyclohexane ring in form II were presumably due to the flip-flop motion (correlation time being 10^{-4}—10^{-5} s) between the chair and boat forms. Results from the X-ray diffraction pattern and the crystal density also suggested that "free volume" for the flexible motion of the cyclohexane ring was present for form II.

Key words candesartan cilexetil; polymorph; IR spectrometry; solid-state NMR

Crystal polymorphism is one of the most important physicochemical properties in pharmaceutics. Polymorphic forms have their own characteristics of solubility, bioavailability, and physical/chemical stability.[1,2] Several techniques for solid-state measurements have been reported in the study of polymorph: microscopy, IR spectroscopy,[3] differential scanning calorimetry (DSC),[4—6] powder X-ray diffractometry (XRD),[7,8] and solid-state NMR.[9—15] Among such techniques, solid-state NMR is a non-destructive one, and has the ability to probe the individual chemical environment of each atom.

In pharmaceutical research, solid-state NMR has also been used for the solid-state interaction with excipients,[16—18] the behavior of water in pharmaceutical solids,[19,20] and a stability study.[21]

TCV-116 ((±)-1-(cyclohexyloxycarbonyloxy)ethyl 2-ethoxy-1-[[2′-(1*H*-tetrazol-5-yl)biphenyl-4-yl]methyl]-1*H*-benzimidazole-7-carboxylate) is a beneficial agent for hypertension, and a prodrug which is esterificated at the carboxyl group of the active compound (CV-11974) by the cyclohexyloxycarbonyloxyethyl group.[22,23] TCV-116 is the racemic compound having an asymmetric carbon in the cyclohexyloxycarbonyloxyethyl group, and two stable racemic crystals have been obtained although their homochiral crystals are low crystalline. In this study, TCV-116 was used for elucidating the nature of crystal polymorph and the physical characterization of TCV-116 was investigated by DSC, powder XRD, IR, and solid-state NMR.

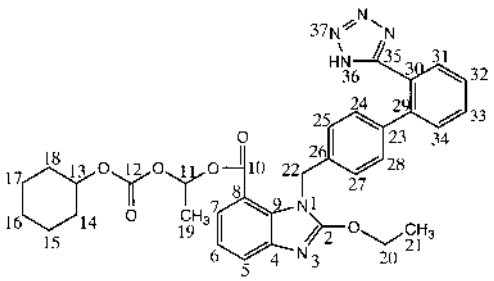

Chart 1. Structure of TCV-116

Experimental

Materials TCV-116 was prepared by Chemical Development Laboratories of Takeda Chemical Industries, Ltd. TCV-116 is usually provided as form I, which is the stable form. The ^{13}C-NMR signal assignment for TCV-116 in dimethylsulfoxide (DMSO)-d_6 is shown in Table 1.

Preparation of Polymorphs and Amorphous Form The relationship among the amorphous form and two identified crystals (form I and form II) of TCV-116 is summarized in Chart 2. The two polymorphs were obtained by recrystallization from solvents. Form I was from several solvents, *e.g.*, a

Table 1. ^{13}C-NMR Assignment for TCV-116

Chemical shift (δ, ppm)	Assignment	Chemical shift (δ, ppm)	Assignment
14.30	C21	126.42	C25, C27
19.07	C19	127.71	C32
22.86	C15	129.01	C24, C28
22.90	C17	130.50	C34
24.53	C16	130.55	C31
30.71	C18	130.95	C33
30.74	C14	131.29	C9
46.24	C22	136.06	C26
66.69	C20	138.26	C23
76.74	C13	140.88	C29
91.86	C11	141.74	C4
114.07	C8	151.90	C12
120.82	C6	154.61	C35
122.43	C5	158.36	C2
123.33	C7, C30	163.54	C10

In DMSO-d_6 (internal standard, trimethylsilane).

* To whom correspondence should be addressed.

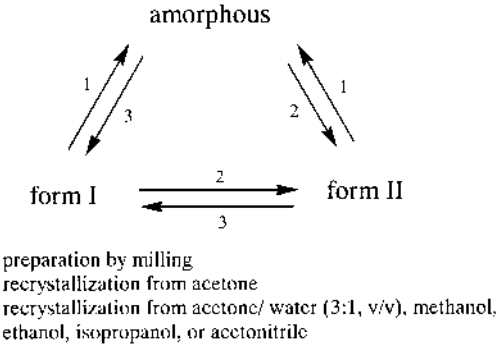

Chart 2. Schematic Diagram of the Solid Forms of TCV-116

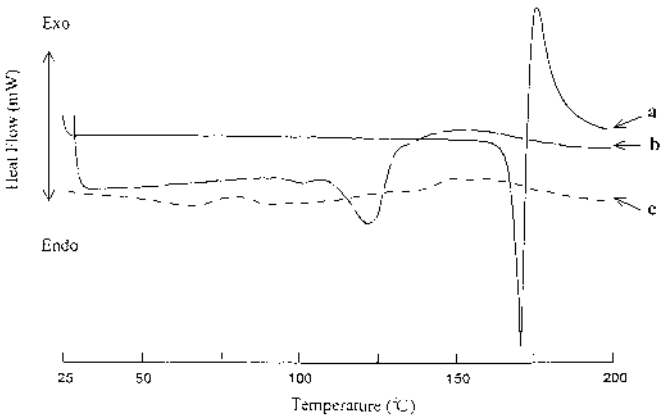

Fig. 1. DSC Thermograms of TCV-116 Heating rate; 5 °C/min
a) Form I, b) form II, c) amorphous form.

mixture of acetone and water (3 : 1, v/v), methanol, ethanol, isopropanol and acetonitrile, while form II was only obtained from acetone. In this study, form I was obtained from a mixture of acetone and water (3 : 1, v/v). The amorphous form of TCV-116 could be prepared from both crystalline forms by milling with a mixer-mill (Spex 8000; Spex industries, Inc., NJ, U.S.A.). TCV-116 in form I, which was stored at −20 °C for 30 min before milling, was immediately milled for 5 min to avoid decomposition. After milling, XRD of the prepared sample was measured. The sample preparation as described above was repeated until amorphous state could be confirmed by XRD.

The content of form I, form II and amorphous form used in this study was 99.4%, 97.1% and 97.7%, respectively. The residual solvent (acetone; 1500 ppm) was determined for TCV-116 in form II. No solvent was detected in either TCV-116 in form I or amorphous form.

Apparatus Thermal Analysis DSC was performed using model DSC-220C (Seiko, Tokyo, Japan) with the heating rate of 5 °C/min under nitrogen stream. DSC temperature scale was calibrated by the indium standard.

Melting Point Melting point was measured by a model MP-21 melting point apparatus (Yamato, Tokyo).

Powder XRD A model RAD-B X-ray diffractometer (Rigaku, Tokyo) with Cu$K\alpha$ radiation was used for the acquisition of XRD patterns. Voltage and current were set 40 kV and 20 mA, respectively. All patterns were scanned over the range 5—45° 2θ angle with a scan rate of 1.5°/min.

Crystal Density The crystal density was measured by a model 1320 autopycnometer (Shimadzu, Kyoto, Japan). After an empty test, the test cell was filled with about 4 g of TCV-116 in form I (form II). The test cell in the pycnometer was sealed, and volatile contaminants were removed by degassing under vacuum. Helium was charged into the test cell, and the volume of helium filling the test cell was measured.

IR Spectroscopy IR spectra were recorded on a model I-5020 Fourier transform IR spectrometer (Hitachi, Tokyo) by the conventional KBr pellet method.

NMR Spectroscopy The ^{1}H-NMR spectrum of TCV-116 in DMSO-d_6 was recorded on an A500 spectrometer (JEOL, Tokyo) with tetramethylsilane as an internal reference. Solid state ^{13}C-NMR was performed on a DSX-200 spectrometer (Bruker, Germany) with a 7 mm (diameter) cross polarization magic angle spinning (CP/MAS) probe and hexamethylbenzene as an external reference.

High-Performance Liquid Chromatography (HPLC) HPLC was used to determine the content of TCV-116. The HPLC equipment was as follows: two pumps (L-6200 and L-6000; Hitachi, Tokyo) equipped with an auto-sampler (AS-4000, Hitachi), an octadecyl silica (ODS) column (YMC Pro C18, 150×4.6 mm i.d., spherical, 5 μm, 120 Å; YMC Co., Ltd., Kyoto), UV-VIS detector (L-4000; Hitachi). The gradient elution was performed from acetonitrile/water/acetic acid (57/43/1, mobile phase A) to acetonitrile/water/acetic acid (90/10/1, mobile phase B) over 30 min, the flow rate was 0.8 ml/min. Absorbance was detected at 254 nm. TCV-116 was dissolved and diluted with the mobile phase A (400 μg/ml).

Gas chromatography (GC) GC was used for the determination of the residual solvent (acetone) of TCV-116 in form I, form II and amorphous form. GC was equipped with a hydrogen flame-ionization detector and a 0.53 mm i.d. ×30 m fused silica capillary column coated with 5 μm chemically cross-linked 5% phenyl–95% methylpolysiloxane (SPB-5; Supelco, Inc., PA, U.S.A.). The carrier gas was helium with a linear velocity of about 35 cm per second. The injection port temperature and the detector temperature were maintained at 180 and 260 °C, respectively. The column temperature was programmed according to the following steps: 35 °C for 10 min, then increased linearly to 175 °C at a rate of 8 °C/min, followed by an increase to 260 °C at a rate of 35 °C/min and held for 16 min. TCV-116 was dissolved and diluted with benzyl alcohol (20 mg/ml). In this procedure, the detection limit was 30 ppm (acetone).

Results and Discussion

Thermal Analysis The melting point of TCV-116 in form I was observed at 163 °C with decomposition, whereas TCV-116 in form II was opaque at near 120 °C. In the amorphous form, the melting point could not be specified. The DSC measurements for all forms were consistent with the results of melting points as shown in Fig. 1. The DSC thermogram of TCV-116 in form I showed a sharp endothermal peak (169 °C) followed by an exothermal peak caused by decomposition. TCV-116 in form II was observed as a shallow endothermal peak at about 120 °C. After DSC measurement, the collected samples were analyzed by HPLC to determine the content of TCV-116 in form II. The sample heated up to 125 °C was decomposed (residual content, 68.6%), although the sample heated up to 80 °C was stable (residual content, 98.8%). Results from the HPLC analysis suggested that TCV-116 in form II began to decompose as well as melting. Therefore, the DSC curve of form II gave a shallow endothermal peak. In amorphous form, samples heated up to 75 °C, 110 °C and 150 °C were also analyzed by HPLC. TCV-116 in amorphous form was already liquid phase at 75 °C, and the residual contents of TCV-116 were 81.3% (at 75 °C), 61.9% (at 110 °C) and 16.0% (at 150 °C). Therefore, TCV-116 in amorphous form transferred first to the liquid phase and decomposed at low temperature, although endothermal and exothermal peaks could not be clearly observed.

Powder X-Ray Diffraction Patterns Figure 2 shows the powder X-ray diffraction patterns of TCV-116 in form I, form II, and amorphous form. These patterns indicated that there were different crystal structures in form I and form II, suggesting the different packing or conformation of TCV-116 molecules in each crystal lattice. The characteristic peaks, 2θ, were observed at 9.82° for TCV-116 in form I and 7.28° in form II. This result suggested that TCV-116 in form II exhibited the large spacing lattice planes compared with form I.

The crystal density of TCV-116 in form I and that in form II were 1.273±0.0018 (mean±S.D.; n=6, R.S.D.=0.14%) and 1.223±0.0012 (mean±S.D.; n=6, R.S.D.=0.10%), re-

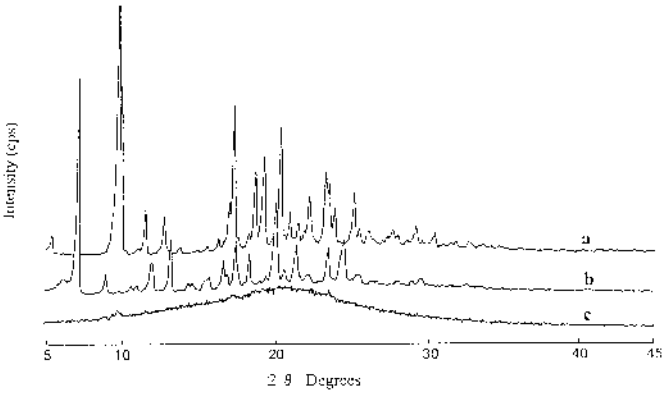

Fig. 2. Powder XRD Patterns of TCV-116
a) Form I, b) form II, c) amorphous form.

Table 2. Crystal Properties of TCV-116 in Form I and Form II

	$2\theta°$	Interplanar spacing (d)	I/I_0	Crystal density
Form I	9.82	9.000	100	1.273 g/cm^3
	17.18	5.157	58	
	18.58	4.772	34	
	19.12	4.638	31	
	20.26	4.380	31	
	23.22	3.828	39	
Form II	7.28	12.133	100	1.223 g/cm^3
	12.04	7.345	42	
	13.20	6.702	50	
	17.36	5.104	57	
	19.96	4.448	73	
	24.34	3.654	53	

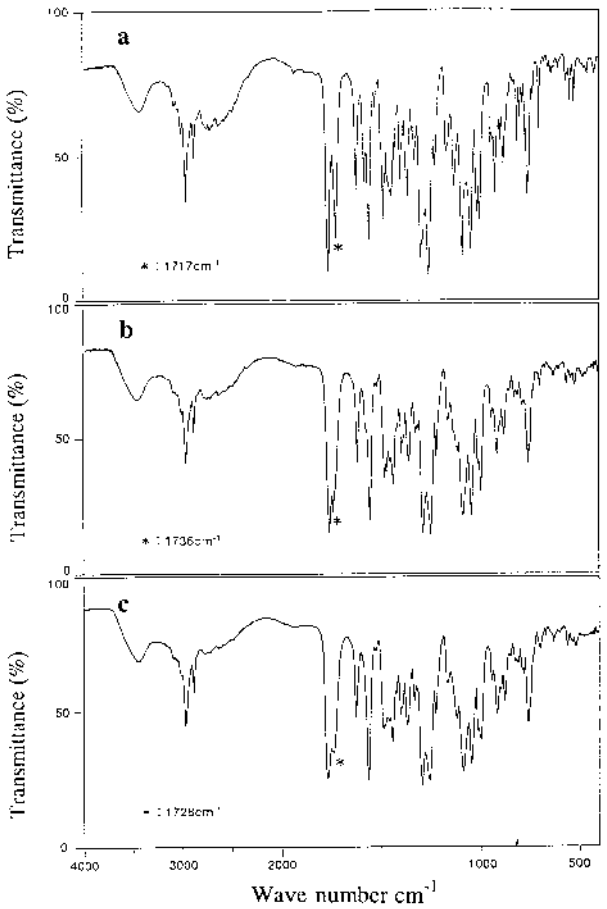

Fig. 3. IR Spectra of TCV-116
a) Form I, b) form II, c) amorphous form.

spectively. Results from the crystal densities of TCV-116 in the two forms, as shown in Table 2, also indicated that molecular packing in the crystals of form II was not dense compared with that of form I.

IR Spectroscopy Figure 3 shows IR spectra of TCV-116 in form I, form II and amorphous form. The great difference among the three spectra was the strong absorption band at 1754—1717 cm^{-1} assigned to the carbonyl stretching vibration. The absorption band observed at 1717 cm^{-1} in form I was shifted to 1736 cm^{-1} in form II, although another carbonyl absorption band was commonly recognized at the same position. These differences in the spectra of TCV-116 between form I and form II suggest that the conformation of cyclohexcyloxycarbonyloxyethyl group of TCV-116 in form II is different from that in form I. In amorphous form, IR spectrum became broad compared to the spectra of forms I and II. The absorption band assigned to the carbonyl stretching vibration was shifted to the middle position (1728 cm^{-1}) of form I (1717 cm^{-1}) and form II (1736 cm^{-1}).

^{13}C CP/MAS NMR Spectra To distinguish molecular structures and dynamics of TCV-116 in these three forms (form I, form II and amorphous form), solid-state NMR spectroscopy was employed. Figure 4 shows ^{13}C CP/MAS spectra of TCV-116 in form I and form II.

The chemical shifts of methyl groups (C_{19}, C_{21}) and the lineshape of cyclohexane ring (C_{13}—C_{18}) were different between these two forms. For the signals of methyl groups (C_{19}, C_{21}), the C_{19} signal in form II was significantly shifted to the lower field compared to that in form I, although the C_{21} signal was scarcely shifted. These results indicated that the relative location of C_{19} in form II was different from that in form I and the dissolved state (free molecule) in DMSO-d_6. ^{13}C CP/MAS spectrum of TCV-116 in amorphous form obtained from form I was the same as that from form II as shown in Fig. 5. In addition, the chemical shifts of TCV-116 in amorphous forms were similar to those of form I. These results also suggested that intermolecular interactions and arrangements (or molecular packing) in the crystal lattice of form II seemed to be different from the other forms.

Effect of Temperature on the ^{13}C CP/MAS Spectra To investigate the effects of temperature on ^{13}C chemical shifts of TCV-116, ^{13}C CP/MAS spectra at various temperatures were obtained. For the spectra of TCV-116 in form I and amorphous form, the chemical shift and the lineshape (see Figs. 4 and 5) were not affected by changing the temperature (data not shown). However, the different spectra were observed for form II with varying temperatures. Figure 6 shows the spectra of form II in the temperature range from −89 °C to 80 °C. Sharp signals due to the cyclohexane ring were obviously both at lower (−89 °C) and higher temperature (80 °C), although the signals became broad and weak at 20 °C and 50 °C (medium temperature range). ^{13}C signals due to the terminal cyclohexane ring (C_{13}—C_{18}) indicate very large temperature dependence, and this phenomenon is found to be reversible in the temperature variation.

It has been pointed out that not only the signal-to-noise

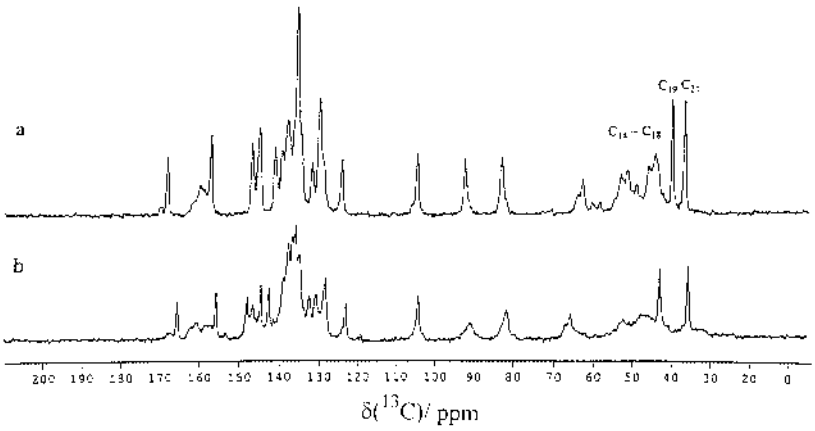

Fig. 4. ^{13}C CP/MAS Spectra of TCV-116 at 20 °C
a) Form I, b) form II.

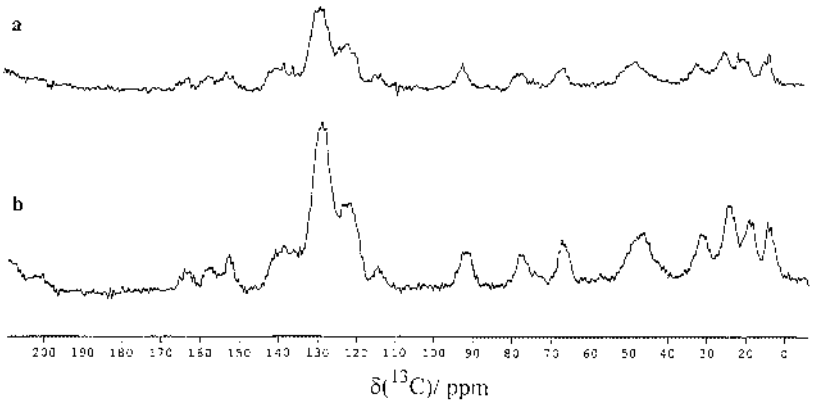

Fig. 5. ^{13}C CP/MAS Spectra of TCV-116 in Amorphous Form at 20 °C
Amorphous forms, a and b were obtained from TCV-116 in form I and form II by milling, respectively.

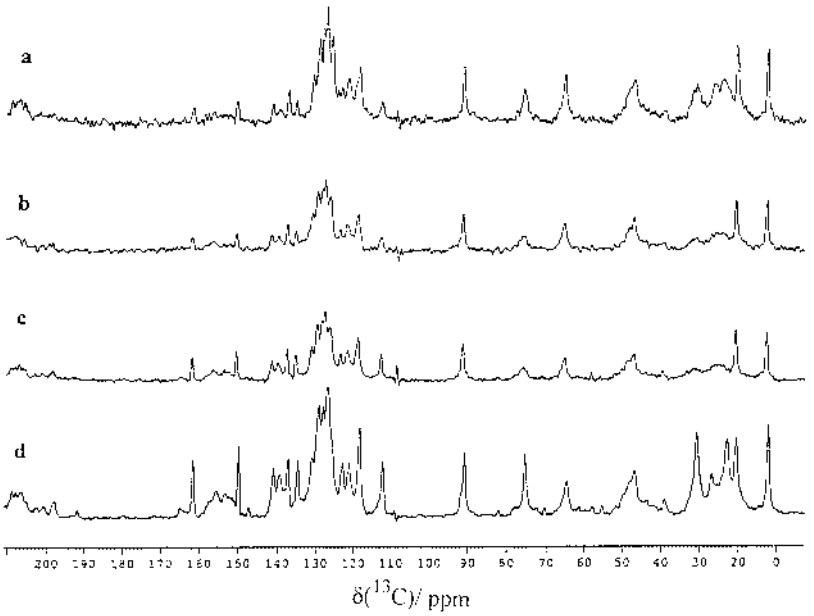

Fig 6. Temperature Variation on ^{13}C CP/MAS Vpectra of TCV-116 in form II
a) 80 °C, b) 50 °C, c) 20 °C, d) −89 °C.

ratio but also line-broadening in CP/MAS measurements are caused by dynamic molecular reorientation which occurs with a similar frequency to the rf-decoupling field.[24] In this case, the temperature dependence of CP/MAS NMR linewidths can be given by

$$\frac{1}{T_2}=\frac{\gamma_H^2\gamma_C^2\hbar^2}{5r^6}\left(\frac{\tau_c}{1+\omega_1^2\tau_c^2}\right) \quad (1)$$

where γ_H and γ_C are the gyromagnetic ratio for ^1H and ^{13}C, respectively, $\hbar$ the Planck constant, τ_c the correlation time of molecular motion, T_2 the spin–spin relaxation time, r the distance between ^1H and ^{13}C, and the protons are subjected to an rf-decoupling of intensity ω_1. According to Eq.1, the linewidth, which equals $1/T_2$, gives a maximum when $\omega_1\tau_c=1$. This condition also corresponds to the minimum of $T_{1\rho}$, spin–lattice relaxation time in the rotating frame. In our normal decoupling intensity, it can be expected that τ_c is 10^{-4}—10^{-5} s. In other words, if the correlation time of molecular motion becomes as fast as 10^{-4}—10^{-5} s in a certain temperature region, the CP/MAS signals for ^{13}C nuclei concerned with the motion become very weak. In the higher temperature region, molecular motion takes place rapidly to satisfy the condition $\omega_1\tau_c\ll1$ (fast motion limit), and in the lower temperature region, it takes place slowly to satisfy the condition $\omega_1\tau_c\gg1$ (slow motion limit). Therefore, we can expect to detect strong signals for both limiting cases. This mechanism of line broadening has been clearly observed in various systems in the solid state.[25,26]

Cyclohexane ring is highly flexible, and it can exist in two interconvertible conformations, the boat and chair forms. At −85 °C, the well-resolved signals (C_{13}—C_{18}) of the stable conformation (chair form) could be observed. At lower temperature (slow motion limit), the cyclohexane ring of TCV-116 in form II can be expected to assume the stable conformation: the chair conformer. In the medium temperature range (20 °C, 50 °C), the shallow signals were observed, suggesting that the conformational change between the chair and boat forms becomes rapid enough to satisfy the condition $\omega_1\tau_c=1$, and then probably averages the different chemical shifts of these two conformers (*ca*. 200 Hz, which corresponds to 5 ms for the correlation time, between C_{16} and C_{15}, C_{17} signals). As the temperature increased further (fast motion limit), the signals became strong and were observed again corresponding to the stable conformer (chair form). These results indicate that the amplitude of this flip–flop motion increases and at last chair–chair conformational change takes place. Therefore, the resolved signals were also observed at high temperature.

In contrast to form II, neither form I nor amorphous form indicated such a temperature dependence on ^{13}C CP/MAS NMR spectra. As you can see, in general, there are two possibilities to explain these phenomena: The molecular motion in these forms is in 1) fast motion limit ($\omega_1\tau_c\ll1$) or 2) slow motion limit ($\omega_1\tau_c\gg1$). Taking into account the XRD data and IR data described above, it is strongly suggested that molecular motion in form I is in the slow motion limit. However, it is not easy to determine the motional state in amorphous form because the resonance lines become very broad as shown in Fig. 5 due to the inhomogeneous crystalline state, although molecular motion in amorphous form is considered to assume the fast motion limit.

Considering the results from XRD and crystal density, as described above (shown in Table 2), the behavior of the cyclohexane ring also implies that the vacant spaces such as "free volume" for the flexible motion are present at the crystalline lattice in form II.

In conclusion, two crystalline forms of TCV-116 were characterized by powder XRD, IR, and solid-state NMR. Different crystalline forms could be distinguished by powder XRD and solid-state NMR, and different comformations in crystalline forms were confirmed by IR and solid-state NMR. The presence of the free volume of TCV-116 in form II is presumed to influence the difference of the physicochemical characterization between form I and form II.

References

1) Ledwidge M. T., Draper S. M., Wilcock D. J., Corrigan O. I., *J. Pharm. Sci*., **85**, 16—21 (1996).
2) Phadnis N. V., Suryanarayanan R., *J. Pharm. Sci*., **86**, 1256—1263 (1997).
3) Loyd G. R., Craig D. Q. M., Smith A., *J. Pharm. Sci*., **86**, 991—996 (1997).
4) Yu L., *J. Pharm. Sci*., **84**, 966—974 (1995).
5) Caira M. R., Easter B., Honiball S., Horne A., Nassimbeni L. R., *J. Pharm. Sci*., **84**, 1379—1384 (1995).
6) Mcmahon L. E., Timmins P., Williams A. C., York P., *J. Pharm. Sci*., **85**, 1064—1069 (1996).
7) Bugay D. E., *Pharm. Res*., **10**, 317—327 (1993).
8) Li R. C., Mayer P. T., Srived J. S., Fort J. J., *J. Pharm. Sci*., **85**, 773—780 (1996).
9) Zhu. H., Khankari K., Padden B. E., Munson E. J., Gleason W. B., Grant D. J. W., *J. Pharm. Sci*., **85**, 1026—1033 (1996).
10) Redenti E., Delcanale M., Amari G., Ventura P., Bacchi A., Pelizzi G., *J. Pharm. Sci*., **84**, 1126—1133 (1995).
11) Stephenson G. A., Borchardt T. B., Byrn S. R., Bowyer J., Bunnell C. A., Snorex S. V., Yu L., *J. Pharm. Sci*., **84**, 1385—1386 (1995).
12) Stephenson G. A., Stowell J. G., Toma P. H., Pfeiffer R. R., Byrn S. R., *J. Pharm. Sci*., **86**, 1239—1244 (1997).
13) Brittain H. G., *J. Pharm. Sci*., **86**, 405—412 (1997).
14) Duddu S. P., Khin-khin A., Grant D. J. W., Suryanarayanan R., *J. Pharm. Sci*., **86**, 340—345 (1997).
15) Ceolin R., Toscani S., Gardette M. F., Agafonov V. N., Dzyabchenko A. V., Bachet B., *J. Pharm. Sci*., **86**, 1062—1065 (1997).
16) Brittain H. G., *Pharmaceutical Technology*, **1997**, 100—108.
17) Sekizaki H., Danjo K., Eguchi H., Yonezawa Y., Sunada H., Otsuka A., *Chem. Pharm. Bull*., **43**, 988—993 (1995).
18) Otsuka T., Yoshioka S., Aso Y., Kojima S., *Chem. Pharm. Bull*., **43**, 122—1223 (1995).
19) Aso Y., Yoshioka S., Terao T., *Chem. Pharm. Bull*., **42**, 398—401 (1994).
20) Oksanen C. A., Zografi G., *Pharm. Res*., **10**, 791—799 (1993).
21) Aso Y., Sufang T., Yoshioka S., Kojima S., *Drug Stability*, **1997**, 237—242.
22) Kubo K., Kohara Y., Yoshimura Y., Inada Y., Shibouta Y., Furukawa Y., Kato T., Nishikawa K., Naka T., *J. Med. Chem*., **36**, 2343—2349 (1993).
23) Noda M., Fukuda R., Matsuo T., Ohta M., Nagano H., Imura Y., Nishikawa K., Shibouta Y., *Kidney Inter. Suppl*., **52**, S136—S139, (1997).
24) Rothwell W. P., Waugh J. S., *J. Chem. Phys*., **74**, 2721 (l981).
25) Wagner G. W., Hanson B. E., *Inorg. Chem*., **26**, 2019 (1987).
26) Eguchi T., Harding R. A., Heaton B. T., Longoni G., Miyagi K., Nähring J., Nakamura N., Nakayama H., Smith A. K., *J. Chem. Soc*., *Dalton Trans*., **1997**, 479—483.